Original article
DOI: https://doi.org/10.18721/JPM.15102

AN ALGEBRAIC TRANSITION MODEL FOR SIMULATION OF TURBULENT FLOWS BASED ON A DETACHED EDDY SIMULATION APPROACH

A. S. Stabnikov ✉, *A. V. Garbaruk*

Peter the Great St. Petersburg Polytechnic University, St. Petersburg, Russia

✉ an.stabnikov@gmail.com

Abstract: A new hybrid RANS/LES method DDES SST KD is proposed, aimed at computations of flows with separation and laminar-turbulent transition in the attached boundary layer. The method is based on a new transition model which uses the SST turbulence model and k-ω KD transition model as a basis. The resulting approach is then tested on a drag crisis problem flows around a circular cylinder and a sphere. The results show that the proposed method is an improvement relative to DDES SST.

Keywords: turbulence, hybrid RANS/LES, DDES, laminar-turbulent transition model, drag crisis

Funding: The reported study was funded by RFBR, project number 19-31-90046.

Citation: Stabnikov A. S., Garbaruk, A. V., An algebraic transition model for simulation of turbulent flows based on a Detached Eddy Simulation approach, St. Petersburg Polytechnical State University Journal. Physics and Mathematics. 15 (1) (2022) 16–29. DOI: https://doi.org/10.18721/JPM.15102

Научная статья
УДК 532.517.4
DOI: https://doi.org/10.18721/JPM.15102

АЛГЕБРАИЧЕСКАЯ МОДЕЛЬ ЛАМИНАРНО-ТУРБУЛЕНТНОГО ПЕРЕХОДА ДЛЯ РАСЧЕТА ТУРБУЛЕНТНЫХ ТЕЧЕНИЙ НА ОСНОВЕ МЕТОДА МОДЕЛИРОВАНИЯ ОТСОЕДИНЕННЫХ ВИХРЕЙ

А. С. Стабников ✉, *А. В. Гарбарук*

Санкт-Петербургский политехнический университет Петра Великого, Санкт-Петербург, Россия

✉ an.stabnikov@gmail.com

Аннотация. Предложен новый глобальный гибридный вихреразрешающий подход DDES SST KD, предназначенный для расчета отрывных течений при наличии перехода в присоединенном пограничном слое. Подход базируется на разработанной авторами модели перехода, основанной на полуэмпирической модели турбулентности SST и алгебраической модели перехода k-ω KD. На примере задачи об обтекании цилиндра и сферы в широком диапазоне чисел Рейнольдса продемонстрировано преимущество предложенного подхода над оригинальным методом DDES SST.

Ключевые слова: турбулентность, вихреразрешающий метод, RANS/LES, DDES, модель ламинарно-турбулентного перехода, кризис сопротивления

Финансирование: Исследование выполнено при финансовой поддержке РФФИ в рамках научного проекта № 90046-31-19.

Для цитирования: Стабников А. С., Гарбарук А. В. Алгебраическая модель ламинарно-турбулентного перехода для расчета турбулентных течений на основе метода моделирования отсоединенных вихрей // Научно-технические ведомости СПбГПУ. Физико-математические науки. 2022. Т. 15. № 1. С. 16–29. DOI: https://doi.org/10.18721/JPM.15102

Introduction

As increasingly efficient computational resources become available, global hybrid eddy-resolving approaches combining the Reynolds-averaged Navier–Stokes equations (RANS) and the Large Eddy Simulation (LES) methods are gaining widespread popularity for simulation of turbulent flows. Some of the most successful are the methods of the DES family (Detached Eddy Simulation), using a standard semi-empirical turbulence model in RANS subdomains of the flow including the attached boundary layers, and a derived subgrid-scale model in the LES-subdomains including the flow recirculation zones. Switching between RANS and LES is performed dynamically during the solution based on the local flow characteristics and the computational mesh. The general consensus [1] is that Delayed Detached Eddy Simulation (DDES) is the method from this family best suited for solving applied problems [2].

Since the Shear Stress Transport (SST) model [3] is considered one of the best, if not the best semi-empirical turbulence model, the methods based on it may prove more accurate than those based on other models. However, the semi-empirical models used to construct hybrid approaches including the SST model typically do not include mechanisms for describing the laminar-turbulent transition in the boundary layer. This can decrease the computational accuracy, since the entire length of the boundary layer is not turbulent in most flows. The turbulent region is generally preceded by a laminar region of some extent, which can significantly affect the overall characteristics of the flow. This effect appears not only at moderate but also at high Reynolds numbers, especially upon separation from a smooth surface. A classic example of the transition effect on separation flow is the drag crisis in bluff bodies, described in detail by Loitsyansky [4]. The crisis is that vortex shedding occurs until the attached boundary layer separates as the Reynolds number increases, which leads to a shift in the separation point and a sharp drop in the drag coefficient.

Thus, the accuracy of hybrid approaches can be improved in some cases by using RANS models capable of accounting for the laminar-turbulent transition (so-called transition models) as a basis.

To date, a large number of transition models have been formulated. Most of them are based on solving differential equations for transport of auxiliary quantities, such as the intermittency γ, the critical Reynolds number Re_θ, the laminar kinetic energy k_l or others. Notably, the existing transition models are still far from perfect, while the SST γ-Re_θ model [5] is regarded as the most accurate, yielding acceptable accuracy for predicting the transition position in diverse types of flows. Four differential equations are solved within this model (two for turbulence characteristics k and ω, as well as two for auxiliary quantities, the intermittence γ and the critical Reynolds number Re_θ). Although the SST γ-Re_θ model offers superior accuracy compared to the standard SST model, as it is capable of describing the transition by different scenarios, it carries higher computational costs necessary to obtain a convergent solution, and in fact sometimes the convergence of the iterative process cannot be achieved at all [6, 7]. These problems are not a specific drawback of the γ-Re_θ model: they are also characteristic of other, less accurate differential transition models. Interestingly, these drawbacks are, so to speak, inherited by hybrid eddy-resolving approaches based on differential transition models as standard RANS models. The same as in the case of RANS, this can lead to computational problems manifesting as the lack of iterative convergence at each time step and increased computational time.

Recently, more and more efforts have been made to develop algebraic transition models, which allow to avoid solving additional differential equations for transition characteristics. These models seem very promising, since they are simpler to use than differential models, provide better convergence and take a relatively small number of additional computations compared to the standard turbulence models on which they are based. Therefore, as algebraic transition models show potential for hybrid approaches, we have concentrated on this subject in the study.

We propose a new hybrid DDES SST KD method combining an algebraic transition model and the transport equations for k and ω as a basis (this approach has been formulated for the first time). The proposed approach comprises the DDES method combined with the shear-layer-adapted (ΔSLA) subgrid length scale, allowing to accelerate the transition to resolved turbulent structures in the separated shear layers, and the SST model complemented with algebraic relations for determining the position of the laminar-turbulent transition from the Kubacki–Dick (KD) k-ω model. Since the ratios of the KD model given in the original study [8] were formulated for Wilcox's k-ω turbulence model [9], they were modified considerably to be used together with the SST model (for details, see the section 'Formulation of the proposed method' below). The

advantages of the approach proposed over the original DDES SST method are illustrated by computational problems on the drag crisis for flow around a sphere and a circular cylinder.

The model and the method were implemented within the framework of the NTS (Numerical Turbulence Simulation), an in-house finite-volume code [10] using the Rogers–Kwak flux-difference splitting [11] to solve incompressible equations of motion, combining a flux-difference splitting scheme for vectors of gas-dynamic flows and the Yanenko–Chorin method for introducing artificial compressibility [12]. The NTS code runs on structured multi-block overset grids (Chimera technique), allowing to adopt schemes with increased approximation order and simulate flows with complex geometry.

The method for approximating non-viscous components of flux vectors in transport equations plays the central role in computations using hybrid RANS-LES approaches. This method determines the dissipative properties of the scheme, which have different requirements in different regions of the flow: the scheme must ensure the stability of the solution in the RANS subdomain, while low-dissipation schemes capable of resolving small-scale turbulence should be introduced in LES subdomains. This study has adopted a hybrid scheme for this purpose [13], functioning as a 3rd-order upwind-biased scheme in the RANS-subdomains and a 4th-order central-difference scheme in the LES-subdomains of the flow.

Formulation of the proposed method

SST KD algebraic transition model. This model is based on modified transport equations for turbulence of the SST model [3]:

$$\begin{cases} \dfrac{\partial k}{\partial t}+\dfrac{\partial\left(u_k k\right)}{\partial x_k}=\gamma P_k+(1-\gamma)P_{sep}-\beta^*\omega k+\dfrac{\partial}{\partial x_k}\left[\left(\nu+\sigma_k\nu_t\right)\dfrac{\partial k}{\partial x_k}\right], \\ \dfrac{\partial \omega}{\partial x_k}+\dfrac{\partial\left(u_k \omega\right)}{\partial x_k}=P_k-\beta\omega^2+\dfrac{\partial}{\partial x_k}\left[\left(\nu+\sigma_\omega\nu_t\right)\dfrac{\partial \omega}{\partial x_k}\right]+2\left(1-F_1\right)\dfrac{\sigma_{\omega 2}}{\omega}\dfrac{\partial k}{\partial x_k}\dfrac{\partial \omega}{\partial x_k}, \end{cases} \tag{1}$$

where k, $m^2 \cdot s^{-2}$, is the turbulent kinetic energy; ω, s^{-1}, is the specific dissipation rate; ν, $m^2 \cdot s^{-1}$, is the kinematic viscosity; ν_t, $m^2 \cdot s^{-1}$, is the turbulent viscosity; u_k, $m \cdot s^{-1}$, are the velocity components; x_k, m, are the coordinate components; t, s, is the time. The explanation for the quantities P_k, P_{sep} will be given below (see Eqs. (8) and (11)).

The function F_1 is found by the expression

$$F_1=\tanh\left(\arg_1^4\right),\ \ \arg_1=\min\left[\max\left(\frac{\sqrt{k}}{\beta^*\omega d_w},\frac{500\nu}{\omega d_w^2}\right),\frac{2k\omega}{d_w^2\left(\nabla k\right)\cdot\left(\nabla\omega\right)}\right], \tag{2}$$

where d_w is the distance to the wall, and the constants of the SST model have the following values:

$$\begin{gathered} \sigma_k=F_1\sigma_{k1}+\left(1-F_1\right)\sigma_{k2},\ \sigma_{k1}=0.85,\ \sigma_{k2}=1.0, \\ \sigma_\omega=F_1\sigma_{\omega 1}+\left(1-F_1\right)\sigma_{\omega 2},\ \sigma_{\omega 1}=0.5,\ \sigma_{\omega 2}=0.856, \\ \beta=F_1\beta_1+\left(1-F_1\right)\beta_2,\ \beta_1=0.075,\ \beta_2=0.0828, \\ \beta^*=0.09,\ \alpha=\beta/\beta^*-\sigma_\omega\kappa^2/\sqrt{\beta^*}. \end{gathered} \tag{3}$$

Eqs. (1) have three differences from the equations of the original SST model; these differences were introduced so that the model could be used together with the KD transition model, where the turbulent viscosity ν_t is divided into two components: small-scale ν_s and large-scale ν_l. Therefore,

$$\nu_t=\nu_s+\nu_l. \tag{4}$$

and $\nu_s = a_s k_s/\max[a_s\omega, F_2 S]$, $\nu_l = a_l k_l/\max[a_l\omega, F_2 S]$;

here

$$k_S = f_{SS}k;\ k_l = k - k_S;\ f_{SS} = \exp\left(-\left(\frac{C_{SS}\nu\Omega}{k}\right)^4\right), \tag{5}$$

$$C_{SS} = C_S\left(1.0 + C_A f_W \psi\right);\ f_W = 1 - \tanh\left(\frac{k}{C_W \nu\omega}\right);$$
$$\psi = \tanh\left(\frac{-\Omega\left(S-\Omega\right)}{C_\psi\left(\beta^*\omega\right)^2}\right), \tag{6}$$

$$F_2 = \tanh\left(\arg_2^2\right),\ \arg_2 = \max\left(2\sqrt{k}\Big/\left(0.09\omega d_w\right), 500\nu\Big/\left(d_w^2\omega\right)\right). \tag{7}$$

(S, Ω are the magnitudes of the strain and swirl velocity tensors, respectively).

The differences mentioned above consist in the following.

1. Generation of turbulent kinetic energy P_k is calculated using small-scale viscosity and kinetic energy:

$$P_k = \min\left(-\overline{u_i'u_j'}\,\partial U_i/\partial x_j, 10\cdot\beta^* k\omega\right), \tag{8}$$

$$\overline{u_i'u_j'} = \frac{2}{3}k_S\delta_{ij} - 2\nu_S S_{ij}. \tag{9}$$

2. The generative term in Eq. (1) for k is multiplied by the intermittency factor γ:

$$P_k \to \gamma P_k. \tag{10}$$

3. The transition to turbulence in the separated laminar boundary layer is described by introducing an additional term $(1-\gamma)P_{sep}$ to Eq. (1) for k, where the quantity P_{sep}, borrowed in a simplified form from the differential model [14], is calculated by the following formulas:

$$P_{sep} = C_{sep}F_{sep}\nu S^2; \tag{11}$$

$$F_{sep} = \min\left(\max\left(\frac{R_V}{2.2A_V} - 1.0, 0.0\right)1.0\right);\ R_V = \frac{d_w^2 S}{\nu}. \tag{12}$$

The intermittency factor included in the model is determined by the following expression:

$$\gamma = \min\left(\max\left(\frac{k}{\nu A_\gamma \Omega} - 1.0, 0.0\right), 1.0\right). \tag{13}$$

The main difference between the algebraic relations used in the proposed method and the original KD model [8] consists in changing the criterion in Eqs. (5) for f_{SS} and (13) for intermittency γ. Furthermore, the model constants were optimized for problems on the transition boundary layer with a T3C-series pressure gradient [15]:

$$A_\gamma = 1.3,\ C_S = 2.0,\ C_A = 1.0,\ C_\psi = 10.0,\ C_W = 5.0,$$
$$C_{sep} = 2.0,\ A_V = 550.0,\ a_1 = 0.31\ \ a_2 = 0.45. \tag{14}$$

The SST KD model constructed was tested in RANS simulations for 2D problems, where the laminar-turbulent transition plays a major role, confirming that the model proposed yields significantly better accuracy than the original KD k-ω model [8].

DDES SST KD method. The proposed algebraic model of the SST KD transition was combined with the DDES method [2] to make up a basis for the DDES SST KD method, intended for computing separated flows in the presence of a laminar-turbulent transition in the attached boundary layer. The proposed method uses the DDES version introducing a shear-layer-adapted subgrid length scale (DDES ΔSLA [16]). This modification of the subgrid scale is aimed at accelerating the transition to well-developed three-dimensional turbulence in the initial regions of the shear layers and allows significantly increasing the simulation accuracy for separated flows without increasing the computational mesh and, as a result, the computational costs.

The transition model was additionally modified to function within the eddy-resolving method, restricting the transition model outside the boundary layer:

$$\gamma = 1.0 \text{ for } F_1 < 0.9, \tag{15}$$

where F_1 is the function of the SST model (see Eq. (2)).

Application of the developed approach to predicting the drag crisis

Drag resistance for flow around a cylinder. We consider unsteady cross-flow of incompressible fluid around a circular cylinder in the range of Reynolds numbers from $5.0 \cdot 10^4$ to $1.2 \cdot 10^6$; the number is constructed from the diameter D_c of the cylinder and the freestream velocity U_0 ($\mathrm{Re} = D_c U_0/\nu$).

This interval completely covers the drag crisis, which is observed within the range $1.3 \cdot 10^5 < \mathrm{Re} < 10 \cdot 5.0^5$ [17].

Table 1

Boundary conditions for turbulence characteristics in the problem on flow around a cylinder

Re, 10^4	ν_t/ν	Tu, %
5.0	0.30	0.40
8.0	0.30	0.55
10	0.36	0.60
13	0.45	0.64
17	0.56	0.73
20	0.65	0.77
25	0.79	0.95
30	0.94	1.00
40	1.25	1.02
50	1.55	1.15
70	2.16	1.35
90	2.75	1.55
120	3.65	1.70

Notations: Re is the Reynolds number, ν_t is the turbulent viscosity, ν is the kinematic viscosity, Tu is the turbulent intensity.

The computational domain is a cylinder with a radius of $25D_c$, where D_c is the diameter of the streamlined cylinder, centered at $(x, y) = (0.0, 0.0)$. The length of the computational domain in the transverse direction z is $L_z = 5\ D_c$, which is greater than the quantity πD_c commonly used in such computations (see, for example, [18, 19]), and should not adversely affect the result.

Because the SST model assumes that the turbulent kinetic energy decreases (dissipates) in homogeneous turbulent flow, generally, so that the turbulent characteristics in the vicinity of the streamlined body correspond to certain required values, the boundary conditions for the equations of the turbulence model have to be adjusted. Such values can be obtained at the inlet to the computational domain from the analytical solution to the equations of the SST model in homogeneous flow by the following formulas:

$$k = c_2 \left(\beta x + c_1\right)^{\frac{\beta^*}{\beta}}, \tag{16}$$

$$\omega = \frac{1}{\beta x + c_1}, \tag{17}$$

where x is the coordinate along the flow in free stream; c_1, c_2 are the integration constants obtained from boundary values; the values of constants β and β^* are given above.

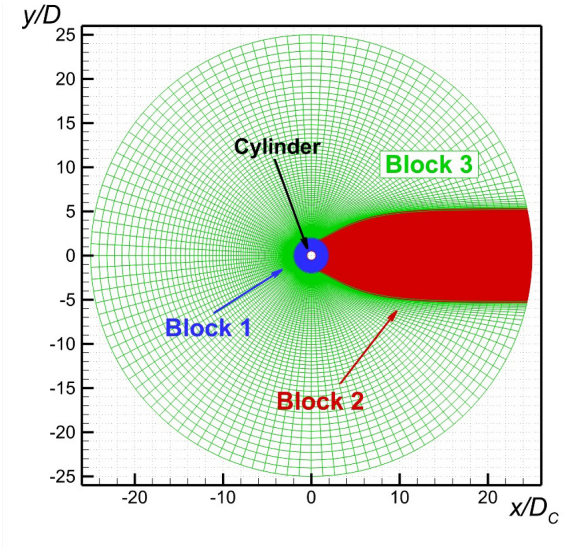

Fig. 1. Three blocks of the computational meshes (shown in different colors) in the problem of flow around a circular cylinder (section $z = 0$)

The equations do not have a finite analytical solution for sufficiently large longitudinal dimensions of the computational domain. In such cases, the turbulence characteristics are 'frozen' to a certain point upstream of the body, then 'released' and dissipated to the required values.

The turbulent intensity Tu = 0.45% (Tu = $100[(2/3)P_k]1/2/U_0$) is generated in this problem in the vicinity of the cylinder's middle section, the turbulence characteristics were frozen to the section $x = 2–D_c$ and their inlet values were calculated by Eqs. (16), (17) (Table 1).

Constant pressure was given at the outlet boundary, and no-slip and impermeability conditions $u_w = v_w = w_w = 0$ were imposed on the cylinder surface. Standard conditions for the SST model were imposed for turbulent characteristics on the wall:

$$k_w = 0,\ \omega_w = 10\frac{6\nu}{\beta_1\Delta_1^{\,2}},$$

where Δ_1 is the size of the first near-wall spacing of the mesh.

Finally, periodic boundary conditions were imposed in the transverse direction.

The computational meshes consisted of three blocks (Fig. 1). The first block contained a refined mesh for computing high gradients of the quantities near the cylinder surface, the second one was refined for computing the wake behind the cylinder. The third block contained unperturbed homogeneous flow without unsteady fluctuations and the coarsest mesh.

A total of three meshes were constructed for computations with different ranges of Reynolds numbers, characterized by the magnitude of the first near-wall spacing: I, II, and III (Table 2).

The time step Δt was equal to $5\cdot10^{-3}\cdot D_c/U_0$, maintaining the value of the Courant–Friedrichs–Lewy (CFL) criterion below unity in the separation zone in the cylinder wake. The solution was averaged after the flow was stabilized over time intervals of about $50\cdot D_c/U_0$.

Fig. 2 compares the simulated dependences obtained for the drag coefficient $C_D = F_x/[(5/2)\rho U_0^2]$ (F_x is the drag force acting on the cylinder, ρ is the density) versus the Reynolds number with the experimental data [20–26].

Table 2

Parameters of computational meshes in the problem on flow around a cylinder

#	Re range, 10^4	Block size			Total number of cells
		Block 1	Block 2	Block 3	
I	5.0–20	512×161×60	200×184×256	131×101×52	56,270,732
II	25–60	512×191×560	200×184×256	131×101×52	64,872,332
III	70–120	512×221×560	200×184×256	131×101×52	73,473,932

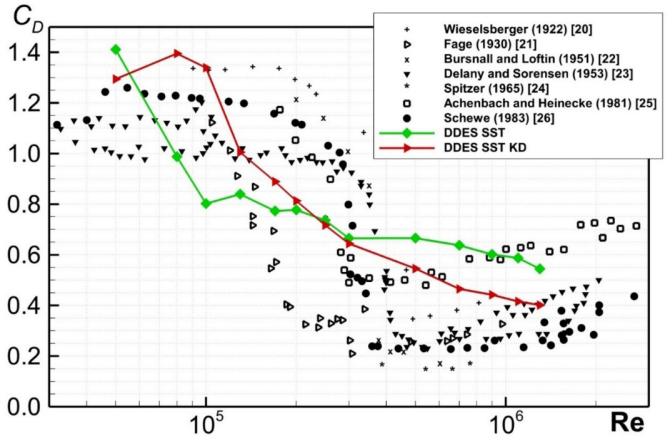

Fig. 2. Simulated curves (solid lines) of the drag coefficient in a circular cylinder as a function of the Reynolds number compared with the experimental data (symbols) [20–26]

This flow clearly confirms the advantage of the proposed hybrid method over the original DDES SST approach. Evidently, the computed drag coefficients obtained by the transition model turn out to be closer to the experimental values. However, complete agreement with the experimental data could not be achieved; in particular, the decrease in the computed drag coefficient in the vicinity of the critical Reynolds number is much slower than in the experimental dependences. The reasons for this behavior require further study and are beyond the scope of our paper.

Drag crisis for flow around a sphere. We consider unsteady cross-flow of incompressible fluid around a sphere in the range of Reynolds numbers from $5.0 \cdot 10^4$ to $4.0 \cdot 10^5$; the number is constructed from the diameter D_s of the sphere and the freestream velocity U_0 ($\mathrm{Re} = D_s U_0/\nu$)

The computational domain is a sphere with a radius of $20D_s$. The boundary conditions were imposed similarly to the solution of the problem on the flow around a cylinder. The only difference was in the inlet values chosen for the turbulence characteristics: they were tailored to provide a turbulence intensity of 0.45% in the vicinity of the sphere's middle section (Table 3).

Table 3

Boundary conditions for turbulence characteristics in the problem on flow around a sphere

Re, 10^4	ν_t/ν	Tu, %
5.0	0.35	1.2
10	0.70	1.2
20	1.40	1.4
40	2.8	1.6
60	4.2	1.7
100	7.0	1.9

The notations are identical to those given in Table 1

The computational mesh consisted of six blocks (Fig. 3). Blocks from 1 to 3 were adjacent to the surface of the sphere and are characterized by small mesh spacings (514 cells per sphere circumference), while the mesh spacings were about 3 times larger in the outer blocks (4 to 6). Blocks 1 and 4 have a cylindrical shape and are characterized by axial symmetry relative to the axis x (Fig. 3,*b*). The remaining mesh blocks have the shape of a truncated pyramid, allowing to avoid unreasonable clustering in the vicinity of the symmetry axis of the 1st and 4th blocks (Fig. 4).

The mesh spacings were refined to the surface of the sphere and in the vicinity of the wake. The same as in the solution to the problem on flow around a cylinder, we constructed a series of meshes for computations at different Reynolds numbers, varying by the first near-wall spacing. The total number of cells in the mesh was about 16 million. A series of preliminary computations carried out by the DDES SST and DDES SST KD methods at $\mathrm{Re} = 1.0 \cdot 10^5$ indicate that refining the mesh by 1.5 times in each direction (this mesh contains is about 46 million cells) does not change the time-averaged solution.

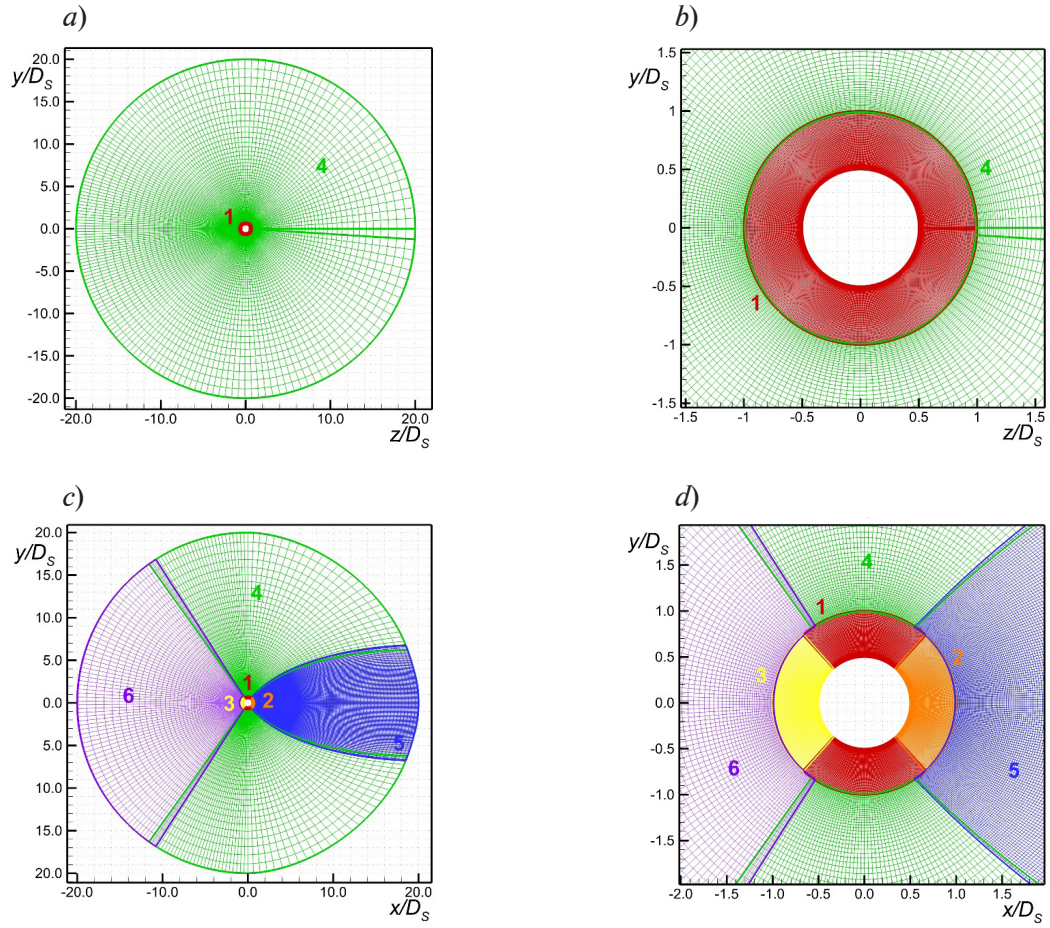

Fig. 3. Blocks of computational meshes (numbered and marked by different colors) for the problem on flow around a sphere. The figure shows sections $z = 0$ (*a*, *b*) and $x = 0$ (*c*, *d*); *b*, *d* are enlarged images of the middle sections in graphs *a* and *c*, respectively

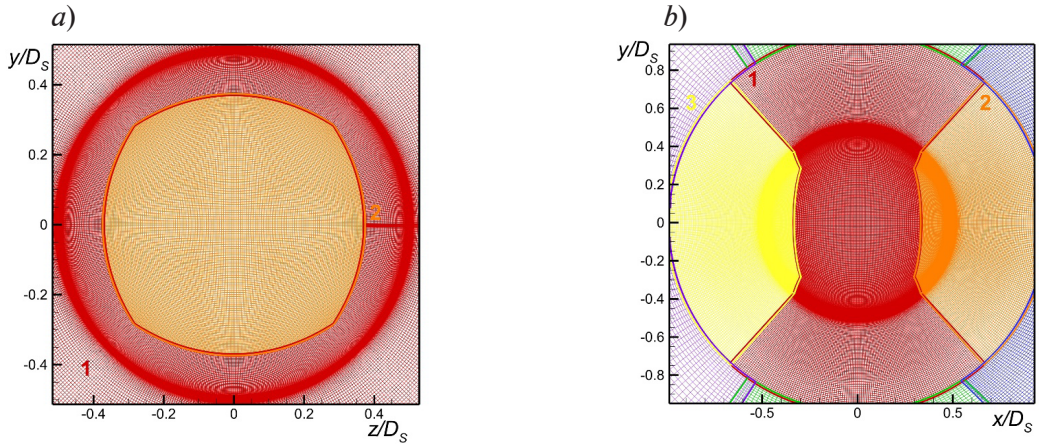

Fig. 4. Computational meshes in sections $x = 0$ (*a*) and $z = 0$ (*b*) for the problem on flow around a sphere. Surface meshes are projected on the corresponding sections

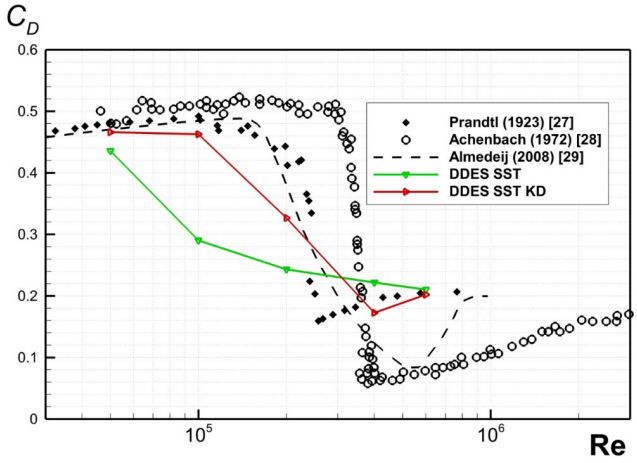

Fig. 5. Simulated curves (solid lines) of the sphere's drag coefficient as a function of the Reynolds number compared with the experimental data (symbols) [27–28] and empirical correlations [29]

The time step was taken equal to $\Delta t = 10{\cdot}5^{-3} D_s/U_0$, providing, the same as in the problem of the cylinder, the value of the Courant number CFL < 1 in the separation zone behind the sphere. Additional computations confirmed that refining the time step does not change the time-averaged solution. The solution was averaged after the flow was stabilized over time intervals of about $50{\cdot}D_s/U_0$.

Fig. 5 compares the simulated dependences obtained for the drag coefficient $C_D = F_x/[(1/2)\rho U_0^2 \cdot (4/1)\pi D_s^2]$ versus the Reynolds number with the experimental data (F_x is the drag force acting on the sphere).

The computational results were compared with the experimental data presented in [27–28] and empirical correlations in [29].

First of all, we should note that the proposed method considerably improves the computational accuracy for all the values of the Reynolds number considered. The original DDES SST method predicts virtually no decrease in the drag coefficient associated with the drag crisis as the Reynolds number increases in the range $1{\cdot}10^5 < \mathrm{Re} < 10{\cdot}4^5$, while the proposed method offers a qualitative description. At the same time, the computational results obtained by the proposed method differed somewhat from the experimental data, which is primarily manifested (the same as in the problem of on flow around a cylinder), in a slower decrease in the computed drag coefficient in the vicinity of the critical value of the Reynolds number.

Conclusion

We have proposed a new global hybrid eddy-resolving approach intended for computing separated flows with a transition in the attached boundary layer. The approach is based on the transition model we have formulated, based on the semi-empirical SST turbulence model and the k-ω KD algebraic transition model.

The advantages of the proposed approach over the original DDES SST method were illustrated by test problems on flow around a cylinder and a sphere in a wide range of Reynolds numbers.

REFERENCES

1. **Garbaruk A. V.**, Sovremennyye podkhody k modelirovaniyu turbulentnosti [Modern approaches to the turbulence simulation], Polytechnic University Publishing, St. Petersburg, 2016.

2. **Spalart P. R., Deck S., Shur M. L., et al.,** A new version of Detached-Eddy Simulation, resistant to ambiguous grid densities, Theoret. Comput. Fluid Dynamics. 20 (3) (2006) 181–195.

3. **Menter F. R., Kuntz M., Langtry R.,** Ten years of industrial experience with the SST turbulence model, Heat & Mass Transfer. 2003. Vol. 4 (January) (2003).

4. **Loytsyanskiy L.G.,** Mekhanika zhidkosti i gaza [Fluids and gas mechanics], Gostechizdat, Moscow-Leningrad, 1950 (in Russian).

5. **Langtry R. B., Menter F. R.,** Correlation-based transition modeling for unstructured parallelized computational fluid dynamics codes, AIAA Journal. 2009. Vol. 47 (12) (2009) 2894–2906.

6. **Wauters J., Degroote J.,** On the study of transitional low-Reynolds number flows over airfoils operating at high angles of attack and their prediction using transitional turbulence models, Prog. Aerosp. Sci. 103 (November) (2018) 52–68.

7. **Lopes R., Eça L., Vaz G.,** On the numerical behavior of RANS-based transition models, J. Fluids Eng. 142 (5) (2020) 051503.

8. **Kubacki S., Dick E.,** An algebraic model for bypass transition in turbomachinery boundary layer flows, Int. J. Heat Fluid Flow. 58 (April) (2016) 68–83.

9. **Wilcox D. C.,** Formulation of the k-ω turbulence model revisited, AIAA Journal. 46 (11) (2008) 2823–2838.

10. **Shur M., Strelets M., Travin A.,** High-order implicit multi-block Navier –Stokes code: Ten-years experience of application to RANS/DES/LES/DNS of turbulent flows (invited lecture), In: Proceeding of the 7th Symposium on Overset Composite Grids and Solution Technology, Oct. 5–7, Huntington Beach, USA, 2004.

11. **Rogers S., Kwak D.,** An upwind differencing scheme for the time-accurate incompressible Navier – Stokes equations, In: Proceeding of the 6th Applied Aerodynamics Conference, American Institute of Aeronautics and Astronautics, Williamsburg, USA.1988, November, Rep. No. NASA-TM-101051.

12. **Chorin A. J.,** A numerical method for solving incompressible viscous flow problems, J. Comput. Phys. 2 (1) (1967) 12–26.

13. **Travin A., Shur M., Strelets M., Spalart P. R.,** Physical and numerical upgrades in the Detached-Eddy Simulation of complex turbulent flows, In book: Advances in LES of Complex Flows, Vol. 65. Ed. by Friedrich R., Rodi W., Springer Netherlands, Dordrecht (2002) 239–254.

14. **Menter F. R., Smirnov P. E., Liu T., Avancha R.,** A one-equation local correlation-based transition model, Flow, Turb. Combust. 95 (4) (2015) 583–619.

15. **Savill A. M.,** Evaluating turbulence model predictions of transition: An ERCOFTAC special interest group project, Appl. Sci. Res. 51 (1–2) (1993) 555–562.

16. **Probst A., Schwamborn D., Garbaruk A., et al.,** Evaluation of grey area mitigation tools within zonal and non-zonal RANS-LES approaches in flows with pressure induced separation, Int. J. Heat Fluid Flow. 68 (December) (2017) 237–247.

17. **Smith A. M. O., Gamberoni N.,** Transition, pressure gradient and stability theory, Techn. Rep. ES-26388, Douglas Aircraft Company, El Segundo Division, Santa Monica, California, USA, 1956.

18. **Pereira F. S., Vaz G., Eca L.,** An assessment of scale-resolving simulation models for the flow around a circular cylinder, In: Proc. Eighth Int. Symp. Turbulence, Heat and Mass Transfer (THMT-15), Sept. 15–18, Begellhouse, Sarajevo, Bosnia and Herzegovina (2015) 295–298.

19. **Pereira F. S., Vaz G., Eça L.,** Flow past a circular cylinder: A comparison between RANS and hybrid turbulence models for a low Reynolds number, In: Proc. ASME 2015: 34th Int. Conf. Ocean, Offshore & Arctic Eng., May 31–June 5, 2015, St. John's, Newfoundland, Canada. Vol. 2: CFD and VIV, ASME, 2015. P. No. OMAE2015-41235, V002T08A006.

20. **Wieselsberger C.,** New data on the laws of fluid resistance, Tech. Rep. Number NACA-TN-84, NACA, 1922, March 1, ID 19930080855.pdf.

21. **Fage A.,** The drag of circular cylinders and spheres at high values of Reynolds number (Tech. Rep.), Reports & Memoranda, No. 1370, Aeronautical Research Commettee, London, May, 1930.

22. **Bursnall W., Loftin L. K. Jr.,** Experimental investigation of the pressure distribution about a yawed circular cylinder in the critical Reynolds number range, Tech. Rep. NACA-TN-2463, NACA, Washington, September, 1951.

23. **Delany N., Sorensen N.** Low-speed drag of cylinders of various shapes // Tech. Rep. NACA TN-3038, NACA, Washington, 1953.

24. **Spitzer R.,** Measurements of unsteady pressures and wake fluctuations for flow over a cylinder at supercritical Reynolds number, Ph.D. thesis, California Institute of Technology, Pasadena, USA,1965.

25. **Achenbach E., Heinecke E.,** On vortex shedding from smooth and rough cylinders in the range of Reynolds numbers 6×10^3 to 5×10^6, J. Fluid Mech. 109 (August) (1981) 239–251.

26. **Schewe G.,** On the force fluctuations acting on a circular cylinder in crossflow from subcritical up to transcritical Reynolds numbers, J. Fluid Mech. 133 (1983) 265–285.

27. **Prandtl L.,** Ergebnisse der Aerodynamischen Versuchsanstalt zu Götingen, II. Lieferung. Der induzierte Widerstand von Mehrdeckern (1923) 9–16.

28. **Achenbach E.,** Experiments on the flow past spheres at very high Reynolds numbers, J. Fluid Mech. 54 (3) (1972) 565–575.

29. **Almedeij J.,** Drag coefficient of flow around a sphere: Matching asymptotically the wide trend, Powder Technol. 186 (3) (2008) 218–223.

СПИСОК ЛИТЕРАТУРЫ

1. **Гарбарук А. В.** Современные подходы к моделированию турбулентности. СПб.: Изд-во Политехнического ун-та, 2016. 233 с.

2. **Spalart P. R., Deck S., Shur M. L., Squires K., Strelets M., Travin A.** A new version of Detached-Eddy Simulation, resistant to ambiguous grid densities // Theoretical Computational Fluid Dynamics. 2006. Vol. 20. No. 3. Pp. 181–195.

3. **Menter F. R., Kuntz M., Langtry R.** Ten years of industrial experience with the SST turbulence model // Heat and Mass Transfer. 2003. Vol. 4. January.

4. **Лойцянский Л. Г.** Механика жидкости и газа. Москва-Ленинград: Гостехиздат, 1950. 676 с.

5. **Langtry R. B., Menter F. R.** Correlation-based transition modeling for unstructured parallelized computational fluid dynamics codes // AIAA Journal (American Institute of Aeronautics and Astronautics). 2009. Vol. 47. No. 12. Pp. 2894–2906.

6. **Wauters J., Degroote J.** On the study of transitional low-Reynolds number flows over airfoils operating at high angles of attack and their prediction using transitional turbulence models // Progress in Aerospace Sciences. 2018. Vol. 103. November. Pp. 52–68.

7. **Lopes R., Eça L., Vaz G.** On the numerical behavior of RANS-based transition models // Journal of Fluids Engineering. 2020. Vol. 142. No. 5. P. 051503.

8. **Kubacki S., Dick E.** An algebraic model for bypass transition in turbomachinery boundary layer flows // International Journal of Heat and Fluid Flow. 2016. Vol. 58. April. Pp. 68–83.

9. **Wilcox D. C.** Formulation of the k-ω turbulence model revisited // AIAA Journal. (American Institute of Aeronautics and Astronautics). 2008. Vol. 46. No. 11. Pp. 2823–2838.

10. **Shur M., Strelets M., Travin A.** High-order implicit multi-block Navier–Stokes code: Ten-years experience of application to RANS/DES/LES/DNS of turbulent flows (invited lecture) // Proceeding of the 7th Symposium on Overset Composite Grids and Solution Technology. October 5–7, Huntington Beach, USA. 2004.

11. **Rogers S., Kwak D.** An upwind differencing scheme for the time-accurate incompressible Navier – Stokes equations // Proceeding of the 6th Applied Aerodynamics Conference. Williamsburg, USA.: American Institute of Aeronautics and Astronautics, 1988, November. Report No. NASA-TM-101051.

12. **Chorin A. J.** A numerical method for solving incompressible viscous flow problems // Journal of Computational Physics. 1967. Vol. 2. No. 1. Pp. 12–26.

13. **Travin A., Shur M., Strelets M., Spalart P. R.** Physical and numerical upgrades in the Detached-Eddy Simulation of complex turbulent flows // Advances in LES of Complex Flows. Vol. 65. Edited by Friedrich R., Rodi W. Dordrecht: Springer Netherlands, 2002. Pp. 239–254.

14. **Menter F. R., Smirnov P. E., Liu T., Avancha R.** A one-equation local correlation-based transition model // Flow, Turbulence and Combustion. 2015. Vol. 95. No. 4. Pp. 583–619.

15. **Savill A. M.** Evaluating turbulence model predictions of transition: An ERCOFTAC special interest group project // Applied Scientific Research. 1993. Vol. 51. No. 1–2. Pp. 555–562.

16. **Probst A., Schwamborn D., Garbaruk A., Guseva E., Shur M., Strelets M., Travin A.** Evaluation of grey area mitigation tools within zonal and non-zonal RANS-LES approaches in flows with pressure induced separation // International Journal of Heat and Fluid Flow. 2017. Vol. 68. December. Pp. 237–247.

17. **Smith A. M. O., Gamberoni N.** Transition, Pressure Gradient and Stability Theory. Technical Report ES-26388. Santa Monica, California, USA: Douglas Aircraft Company, El Segundo Division, 1956. 59 p.

18. **Pereira F. S., Vaz G., Eca L.** An assessment of scale-resolving simulation models for the flow around a circular cylinder // Proceeding of the Eighth International Symposium on Turbulence Heat and Mass Transfer (THMT-15), September 15–18. Sarajevo, Bosnia and Herzegovina: Begellhouse, 2015. Pp. 295–298.

19. **Pereira F. S., Vaz G., Eça L.** Flow past a circular cylinder: A comparison between RANS and hybrid turbulence models for a low Reynolds number // Proceeding of the ASME 2015: 34th International Conference on Ocean, Offshore and Arctic Engineering, May 31–June 5, 2015, St. John's, Newfoundland, Canada. Vol. 2: CFD and VIV. American Society of Mechanical Engineers, 2015. Paper No. OMAE2015-41235, V002T08A006 (11 p.).

20. **Wieselsberger C.** New data on the laws of fluid resistance. Tech. Rep. Number NACA-TN-84. Work of the US Gov. Public Use Permitted, 1922, March 1. ID 19930080855.pdf.

21. **Fage A.** The drag of circular cylinders and spheres at high values of Reynolds number // Tech. Rep., Reports & Memoranda, No. 1370. London: Aeronautical Research Commettee, May, 1930. 12 p.

22. **Bursnall W., Loftin L. K. Jr.** Experimental investigation of the pressure distribution about a yawed circular cylinder in the critical Reynolds number range // Tech. Rep. NACA-TN-2463. Washington: National Advisory Committee for Aeronautics (NACA), September, 1951. 34 p.

23. **Delany N., Sorensen N.** Low-speed drag of cylinders of various shapes // Tech. Rep. NACA TN-3038, Washington: National Advisory Committee for Aeronautics (NACA), 1953. 36 p.

24. **Spitzer R.** Measurements of unsteady pressures and wake fluctuations for flow over a cylinder at supercritical Reynolds number. Ph.D. thesis, Pasadena (USA): California Institute of Technology, 1965. 93 p.

25. **Achenbach E., Heinecke E.** On vortex shedding from smooth and rough cylinders in the range of Reynolds numbers 6×10^3 to 5×10^6 // Journal of Fluid Mechanics. 1981. Vol. 109. August. Pp. 239–251.

26. **Schewe G.** On the force fluctuations acting on a circular cylinder in crossflow from subcritical up to transcritical Reynolds numbers // Journal of Fluid Mechanics. 1983. Vol. 133. Pp. 265–285.

27. **Prandtl L.** Ergebnisse der Aerodynamischen Versuchsanstalt zu Götingen. II. Lieferung. Der induzierte Widerstand von Mehrdeckern, 1923. S. 9–16.

28. **Achenbach E.** Experiments on the flow past spheres at very high Reynolds numbers // Journal of Fluid Mechanics. 1972. Vol. 54. No. 3. Pp. 565–575.

29. **Almedeij J.** Drag coefficient of flow around a sphere: Matching asymptotically the wide trend // Powder Technology. 2008. Vol. 186. No. 3. Pp. 218–223.

THE AUTHORS

STABNIKOV Andrey S.
Peter the Great St. Petersburg Polytechnic University
29 Politechnicheskaya St., St. Petersburg, 195251, Russia
an.stabnikov@gmail.com
ORCID: 0000-0001-7011-6197

GARBARUK Andrey V.
Peter the Great St. Petersburg Polytechnic University
29 Politechnicheskaya St., St. Petersburg, 195251, Russia
agarbaruk@cfd.spbstu.ru
ORCID: 0000-0002-2775-9864

СВЕДЕНИЯ ОБ АВТОРАХ

СТАБНИКОВ Андрей Сергеевич – *аспирант высшей школы математики и вычислительной физики Санкт-Петербургского политехнического университета Петра Великого, Санкт-Петербург, Россия.*

195251, Россия, г. Санкт-Петербург, Политехническая ул., 29
an.stabnikov@gmail.com
ORCID: 0000-0001-7011-6197

ГАРБАРУК Андрей Викторович – *доктор физико-математических наук, доцент высшей школы математики и вычислительной физики Санкт-Петербургского политехнического университета Петра Великого, Санкт-Петербург, Россия.*

195251, Россия, г. Санкт-Петербург, Политехническая ул., 29
agarbaruk@mail.ru
ORCID: 0000-0002-2775-9864

Received 29.09.2021. Approved after reviewing 29.12.2021. Accepted 10.11.2022.
Статья поступила в редакцию 29.09.2021. Одобрена после рецензирования 29.12.2021. Принята 10.11.2022.